ACADEMIC PRESS

Available online at www.sciencedirect.com
SCIENCE DIRECT®

Journal of Catalysis 218 (2003) 267–279

JOURNAL OF CATALYSIS

www.elsevier.com/locate/jcat

Gas-phase hydrogenation of *o*-xylene over Pt/alumina catalyst, activity, and stereoselectivity

Ahmad Kalantar Neyestanaki,[a] Päivi Mäki-Arvela,[a] Henrik Backman,[a] Hannu Karhu,[a,b] Tapio Salmi,[a] Juhani Väyrynen,[b] and Dmitry Yu. Murzin [a,*]

[a] *Laboratory of Industrial Chemistry, Process Chemistry Group, Åbo Akademi University, Biskopsgatan 8, FIN-20500 Åbo/Turku, Finland*
[b] *Department of Applied Physics, University of Turku, Vesilinnantie 5, FIN-20014 Åbo/Turku, Finland*

Received 19 September 2002; revised 6 January 2003; accepted 30 January 2003

Abstract

The kinetics of the gas-phase hydrogenation of *o*-xylene over Pt/alumina catalysts was studied at 430–520 K, a hydrogen partial pressure of 0.19–0.36, and an *o*-xylene partial pressure of 0.04–0.10. The catalysts were characterized by H_2/*o*-xylene TPD, H_2 chemisorption, energy-dispersive X-ray analysis, and XPS. The stereoisomers, *cis*- and *trans*-1,2-dimethylcyclohexane, were the only reaction products. A reversible maximum in the *o*-xylene hydrogenation activity vs temperature was observed; it was explained by a decrease in the surface concentration of *o*-xylene at higher temperatures. The hydrogenation rate was independent of the *o*-xylene concentration, whereas the reaction orders with respect to hydrogen varied from 0.9 to 3 in the temperature range investigated. The stereoselectivity of the products was found to depend on temperature, reactant concentrations, and platinum precursor. The catalyst prepared from a chlorine-containing precursor exhibited a lower hydrogenation activity and selectivity toward the trans isomer. Chlorine remained on the catalyst surface, even after reduction at 673 K. Dehydrogenation and configurational isomerization of *cis*- to *trans*-1,2-dimethylcyclohexane took place at the same time as hydrogenation. Dehydrogenation and configurational isomerization reactions are enhanced by the presence of residual chlorine on the catalyst surface. The reaction pathway is proposed.

Keywords: *o*-Xylene; Hydrogenation; Gas phase; Stereoselectivity; Dehydrogenation; Epimerization; Catalyst; Platinum; Alumina

1. Introduction

Hydrogenation of aromatic compounds over group VIII metals has attracted considerable attention from the standpoint of theory and application; new environmental legislation strictly limits the aromatic contents of fuels, oils, and solvents. The rate of aromatic hydrogenation is strongly affected by steric factors induced by the substitution of alkyl groups in the aromatic ring. The hydrogenation rate decreases with increasing length of the substituent (benzene > toluene > ethylbenzene > cumene) and as the number of substituents increases (benzene ≫ toluene ∼ xylenes > mesitylene) [1–25]. The kinetics of the gas-phase catalytic hydrogenation of xylenes has been investigated over supported Pd [3,10–12], Ni [13–20], Ru [11,21], and Pt [22–25] catalysts. The relative position of the substituents has a significant effect on the reaction rate, the para position being the most reactive and the ortho position the least reactive (*p*-xylene > *m*-xylene > *o*-xylene).

The rate of the hydrogenation of aromatics is slightly influenced by their concentration, whereas reaction orders of up to 3 have been reported with respect to hydrogen. Lin and Vannice [7–9] studied the performance of platinum on various supports in benzene and toluene hydrogenation. The reaction orders with respect to hydrogen in benzene and toluene hydrogenation were reported to vary from 0.6 to unity at 317–373 K [7,8]. A higher specific activity was observed on acidic supports [7,8]. Similar to benzene and toluene hydrogenation [7–9], a reversible maximum of xylene hydrogenation activity vs temperature was observed [3, 10,13–21,24]. Such behavior can not be attributed to equilibrium [28,29]. The reaction orders with respect to *o*-, *m*-, and *p*-xylene are about the same, varying from −0.3 to 0.4 between 393 and 523 K [13–20]. The reaction order with respect to hydrogen increases with temperature from 0.7 to

* Corresponding author.
E-mail address: dmurzin@abo.fi (D.Y. Murzin).

0021-9517/03/$ – see front matter
doi:10.1016/S0021-9517(03)00070-8

2.6 [13–20] within the same temperature range, suggesting a complex multistep reaction mechanism. The reaction orders with respect to *o*-xylene over Pt/alumina catalysts are reported to vary from 0 to 0.28 at 308–363 K, while the order with respect to hydrogen increases from 1.22 at 308–363 K to 2.5 at 413 K [23–25].

Few studies have addressed the kinetics of the gas-phase hydrogenation of xylenes and the distribution of the stereoisomers among the products over supported Pd [10–12], Ni [13–20], and Pt [22–25] catalysts. Independent of the catalyst used, the *cis*-1,2-dimethylcyclohexane (1,2-DMCH) was the dominant reaction product at lower temperature, whereas the formation of the thermodynamically favored *trans*-1,2-DMCH increased by increasing operation temperature [10,13–21,23,24]. The selectivity toward the trans isomer formation over the supported palladium catalysts was reported to increase with temperature, metal dispersion, and support acidity and in the presence of electron donor molecules such as pyridine [10–12]. A decreased rate of *cis*-1,2-DMCH formation and consequently a higher rate of *trans*-1,2-DMCH formation at higher temperature (300–340 K), as well as an increased selectivity of the thermodynamically favored *trans*-1,2-DMCH with smaller Pt particles, was reported over Pt/alumina [24]. On the other hand, in their study of *o*-, *m*-, and *p*-xylene hydrogenation over supported platinum catalysts, Aramendía et al. [22] did not find that product stereoselectivity was affected by the metal dispersion. The formation of *trans*-1,2-DMCH is usually explained by the rollover mechanism, first introduced by Inuone et al. [30], in which the last double bond to be hydrogenated is isomerized, followed by a rollover of the adsorbed species, which is further hydrogenated to *trans*-1,2-DMCH.

Noble metals are also active in dehydrogenation reactions [31–39]. Dehydrogenation of naphthenes can readily take place on platinum surfaces [31–33,35–39]. Dehydrogenation of cyclohexane and cyclohexadiene takes place rapidly at low temperature and low hydrogen partial pressures because the reaction rate is reported to increase with an increase in the hydrogen-to-hydrocarbon ratio [32] and metal dispersion [34]. However, numerous authors refer to the reaction as being structure-insensitive [35,36]. The dehydrogenation of stereoisomeric dimethylcyclohexane and diethylcyclohexane was studied over Pt, Pd, and Ni [37–39]; the rates of aromatization of *cis*- and *trans*-1,2-DMCH were reported to be the same on platinum, while the *trans* isomer converted slower than the *cis* isomer on Pd and Ni.

There are few studies on xylene hydrogenation over supported platinum catalysts which address kinetics and stereoselectivity [22,24,25]. However, the role of the catalyst precursor and the impact of dehydrogenation and epimerization reactions on the overall rate are not well understood. The present work is focused on the kinetics and the product stereoselectivity of the gas-phase hydrogenation of *o*-xylene over platinum catalysts. The *cis*-to-*trans* epimerization and the dehydrogenation of the products were also investigated.

2. Experimental

2.1. Catalyst preparation

Pt/alumina catalysts were prepared by impregnating a γ-alumina support (LaRoche, Versal GL25, BET surface area of 219 m^2/g) with solutions of hexachloroplatinic acid (Pt/Al_2O_3-Cl) and platinum nitrate (Pt/Al_2O_3-N). The catalysts were washed with de-ionized water, dried, and stored for the activity testing. The Pt content was determined by the direct current plasma technique (Spectraspan IIIA, Spectrometrics).

2.2. Catalyst characterization

The dispersion and mean particle diameters of the metal were determined by hydrogen adsorption at 298 K, using a Sorptomatic 1900 (Carlo Erba Instruments). The dissociative adsorption of hydrogen was employed. The procedures for determining the dispersion and mean metallic particle sizes are given elsewhere [26].

Temperature-programmed desorption (TPD) of hydrogen and *o*-xylene was carried out with an AutoChem 2910 instrument (Micromeritics). The desorbed gases were identified and analyzed by a TC detector and a quadropole mass spectrometer (Omnistar, Baltzer Instruments).

The surface and subsurface composition of the catalysts was investigated by a scanning electron microscope (Leica Cambridge, Stereoscan 360) equipped with an energy-dispersive X-ray analyzer (EDXA) and X-ray photoelectron spectroscopy (Perkin-Elmer 5400). A detailed description of the XPS analysis and the problems associated with the overlapping of the Pt $4f$ and Al $2p$ XP lines are discussed elsewhere [27]. To obtain information on particle sizes of the platinum prior to catalyst reduction, particle size calculations based on the Pt/Al XPS intensity ratio were carried out as described by Davis [40]. Assuming a cubic geometry on a diamond-shaped support and taking the respective particle size determined by the H_2-adsorption technique as a reference, the particle size of the freshly dried samples was determined with good accuracy.

2.3. Catalytic activity measurements

2.3.1. *o*-Xylene hydrogenation

The kinetics of *o*-xylene hydrogenation was studied in a continuous-flow differential tube reactor at a WHSV of 116 h^{-1} and at temperatures of 430–520 K at 10 K intervals at atmospheric pressure. The partial pressures of H_2 (AGA, 99.9999 vol%) and *o*-xylene (Fluka, > 99.5 vol%) were varied from 0.19 to 0.36 bar and from 0.04 to 0.10 bar, respectively, using argon (AGA, 99.9999 vol%) as the make-up gas and maintaining a constant GHSV. The flows were controlled by means of mass-flow controllers (Brooks). The temperature of the catalyst bed was measured by means of a thermocouple; *o*-xylene was pumped by a high-performance

liquid chromatography pump (2150 HPLC pump, LKB Bromma) to an evaporator (Bronkhorst) kept at 443 K and was further driven by argon. All the lines from the evaporator and the reactor were heated. The products were analyzed by a Varian GC equipped with a 60-m HP-1 column (cross-linked methyl siloxane) and FI detector and were further analyzed and confirmed by GC-MS (HP 6890-5973 Instrument). Prior to the experiments, the dried catalysts (125- to 150-μm particles, ca. 60 mg) were reduced in situ in a flow of H_2 at 673 K (unless otherwise stated) for 2 h followed by cooling to the reaction temperature, at which point the reactants were introduced to the catalyst. Standard experiments were carried out to ensure that the kinetics was recorded in the absence of internal and external mass-transfer limitations by testing three different catalyst particle sizes (90–100, 125–150, and 180–250 μm), and four catalyst mass/flow ratios. Conversions were kept below 10%.

2.3.2. 1,2-Dimethylcyclohexane (1,2-DMCH) isomerization/dehydrogenation

The isomerization and dehydrogenation of 1,2-DMCH (as a feedstock) was studied in the same experimental setup as described for the *o*-xylene hydrogenation between 430 and 520 K and at partial pressures for *cis*-1,2-DMCH, *trans*-1,2-DMCH, and hydrogen of 0.77×10^{-3}, 0.14×10^{-3}, and 0.19–0.36 bar, respectively. The mass and particle size of the catalyst and the reduction temperature were the same as those in the *o*-xylene hydrogenation experiments. *n*-Heptane was used for dilution of the feed of 1,2-DMCH. The *cis* and *trans* isomer content of the 1,2-DMCH feed (Fluka > 99.5 vol%) was 84 and 15.3 wt%, respectively.

3. Results

3.1. o-Xylene hydrogenation

The hydrogenation experiments were carried out with a catalyst pre-reduced at 573, 623, and 673 K. The highest steady-state hydrogenation rate was obtained with the catalyst reduced at 673 K. Thus, this temperature was selected for further kinetics experiments. The rates were correlated to the amount of hydrogen desorbed from the H_2 TPD experiments (Table 1). *cis*- and *trans*-1,2-dimethylcyclohexane (1,2-DMCH) were the only hydrogenation products; the *cis*-to-*trans* ratio did not change significantly during the initial deactivation of the catalyst. The reference catalyst prepared from the nitrate salt (1 wt% Pt/Al_2O_3-N) exhibited a much higher activity during xylene hydrogenation (Table 1). Table 2 lists the energy-dispersive X-ray analysis (EDXA) and XPS data of the catalysts. Although the two techniques clearly revealed the presence of surface chlorine species on the Pt/Al_2O_3-Cl catalysts after hydrogen pre-treatment, there were still differences in the Cl:Pt and Pt:Al ratios obtained by both techniques, which will be dealt with in the Discussion section. The chlorine left on the catalyst surface inhibits *o*-xylene hydrogenation (Table 1). A hydrogenation reaction did not take place over the alumina support. Fig. 1 presents a typical kinetic experiment. Catalyst deactivation took place for the first 20 min, after which steady state was reached. The observed time-on-stream deactivation is in good agreement with data reported previously [7,8,13–15,23,24]. The deactivation is reversible, as shown by the fact that hydrogen treatment of the used catalyst at 673 K completely restored the initial activity of the catalyst. The deactivation is due to carbon deposition [41,42]. The reproducibility of the results was ±2%; no volatile compounds were detected, with *cis*- and *trans*-1,2-DMCH being the only products formed. The hydrogenation rate passed through a maximum with increasing operation temperature (Fig. 2).

The reaction orders with respect to the hydrogen and *o*-xylene partial pressures were determined between 430 and 520 K. The reaction order with respect to *o*-xylene was close to zero at all temperatures investigated. The reaction order with respect to hydrogen increased from 1.5 at 430 K to 3 at 520 K (Table 3), showing a similar dependence on hydrogen concentration over a supported Ni/Al_2O_3 catalyst as reported elsewhere [13,15]. The dependence on the hydrogen concentration of the products formed, was, as expected, close to the dependency on the hydrogen concentration in the *o*-xylene hydrogenation (Table 3). The activation energy in the *o*-xylene hydrogenation, calculated from Arrhenius plots, was 93 and −24 kJ/mol in the temperature ranges of 430–460 and 460–520 K, respectively.

The results confirmed an increase in the *cis*-to-*trans* 1,2-DMCH ratio with increasing hydrogen and *o*-xylene concentrations (Figs. 3a and 3b). On the other hand, the *cis*:*trans* ratio decreased at a higher operation temperature (Fig. 4).

Table 1
Comparison of catalysts activity at 460 K (conditions: $p_{H_2} = 0.36$ bar, $p_{o\text{-xyl}} = 0.06$ bar, WHSV $= 116\ h^{-1}$)

Catalyst	Dispersion (%)	Particle diameter (nm)	$T_{red.}$ (K)	Rate (mmol/(g_{Pt} s))	TON $\times 10^3$	*cis*/*trans*	n_{H_2} [a]	H_2 desorbed [b] (mmol/g_{Pt})
1 wt% Pt/Al_2O_3–Cl	95.3	1.06	673	0.409	84.0	1.44	2.3	47.2
1 wt% Pt/Al_2O_3–Cl	95.5	1.06	623	0.204	42.0	1.28	2.3	41.0
1 wt% Pt/Al_2O_3–Cl	96.4	1.06	573	0.118	24.5	1.23	1.8	36.1
1 wt% Pt/Al_2O_3–N	87.9	1.16	673	0.819	181.8	1.08	2.6	43.0
2.7 wt% Pt/Al_2O_3–Cl	75.8	1.34	673	0.236	60.3	1.28	2.3	27.6
4.2 wt% Pt/Al_2O_3–Cl	62.2	1.64	673	0.216	71.1	1.15	2.3	22.2

[a] Reaction order with respect to hydrogen.
[b] First H_2 desorption peak corresponding to the H_2 desorbed from platinum [43] per gram exposed of surface platinum determined from H_2 chemisorption.

Table 2
XPS and EDX analysis of the catalysts

Catalyst	Precursor	$T_{red.}$	EDXA		XPS						
		(K)	Cl/Pt	Cl/Al[b]	Al 2*p*	Pt 4$d_{5/2}$	Cl/Pt	Cl/Al[b]	Cl 2$p_{3/2}$	Pt/Al[b]	Pt size (nm)
Al_2O_3	–	–	–	0.4	73.9	–	–	0.3	197.8	–	–
Al_2O_3	HCl[a]	d	–	3.0	74.0	–	–	1.8	198.3	–	
Al_2O_3	HCl[a]	673			73.9	–	–	1.7	198.6	–	
Pt wire	–	–			–	314.3	–	–	–	–	
1 wt% Pt/Al_2O_3	H_2PtCl_6	d	3.48	1.62	73.9	315.2	5.3	1.5	198.3	0.29	0.73
1 wt% Pt/Al_2O_3	H_2PtCl_6	d, s	–	–	74.0	b	8.3	1.6	198.5	0.19	–
1 wt% Pt/Al_2O_3	H_2PtCl_6	573	3.43	1.44	74.1	314.5	b	1.6	198.4	–	–
1 wt% Pt/Al_2O_3	H_2PtCl_6	623	3.65	1.42	–	–	–	–	–	–	–
1 wt% Pt/Al_2O_3	H_2PtCl_6	673	3.27	1.67	73.9	314.6	9.0	1.8	198.3	0.20	1.06
4.2 wt% Pt/Al_2O_3	H_2PtCl_6	d	3.33	5.78	74.0	315.3	3.1	4.9	198.2	1.5	0.81
4.2 wt% Pt/Al_2O_3	H_2PtCl_6	573	–	–	73.9	314.7	5.3	4.5	198.3	0.85	1.36
4.2 wt% Pt/Al_2O_3	H_2PtCl_6	673	2.5	3.57	73.9	314.5	4.4	3.1	198.4	0.70	1.64
					Al 2*p*	Pt 4$d_{5/2}$	N/Pt	N/Al	N 1*s*	Pt/Al	
1 wt% Pt/Al_2O_3	$Pt(NO_3)_2$	d	–	–	74.3	314.9	1.7	0.55	398.9	0.43	
1 wt% Pt/Al_2O_3	$Pt(NO_3)_2$	673	–	–	74.1	314.2	(3.8)	(1.0)	(399.7)	0.36	

Values in parentheses were affected by the protective N_2 atmosphere during the transfer of the sample to UHV.
[a] Treated in 1 M solution of HCl; d, dried in air at 353 K.
[b] Multiplied by 100; s, sputtered in UHV; b, below detection limit.

The dependency of stereoselectivity on the operation temperature and reactant concentrations is in good agreement with previous work on supported nickel catalysts [13,15,16]. Above 480 K, the rate of formation of the *cis* isomer decreased (Fig. 5). Such a decrease in the amount of the *cis* isomer was reported for the reduction of di-substituted cyclopentenes and cyclohexenes at higher temperatures [44].

Temperature-programmed desorption of *o*-xylene was carried out on pre-reduced (673 K) 1 wt% Pt/Al_2O_3–Cl (Fig. 6). A single desorption pattern of *o*-xylene was observed between 340 and 520 K, with a maximum at around 443 K. The hydrogenolysis products, toluene and benzene, were observed in the same temperature range, following exactly the same desorption pattern as *o*-xylene. Ethene (mass 28), which is formed from the re-combination of the methyl groups, was detected, too. Above 573 K, increased cracking (ethene, methane, and hydrogen evolution) took place. The MS was calibrated for the de-fragmented species.

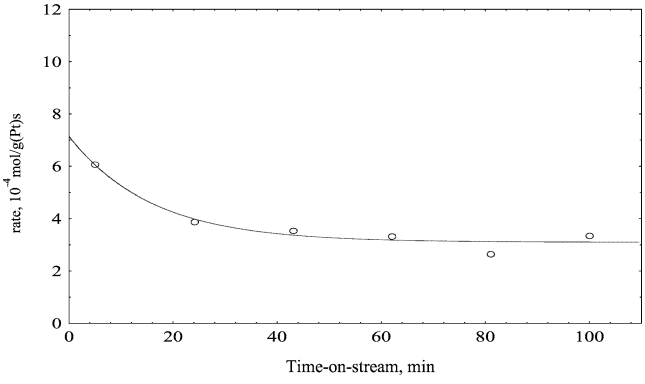

Fig. 1. Time-on-stream hydrogenation activity over 1 wt% Pt/Al_2O_3–Cl catalyst. Conditions: $p_{H_2} = 0.36$ bar, $p_{o\text{-xyl}} = 0.06$ bar, $T = 470$ K.

The hydrogenation activity pattern is very similar to that of the TPD spectra of *o*-xylene (Figs. 2 and 6).

3.2. 1,2-DMCH configurational isomerization and dehydrogenation

Figs. 7a and 7b show the results of *cis–trans* isomerization and dehydrogenation of 1,2-DMCH (with 1,2-DMCH as a feedstock) to *o*-xylene. Dehydrogenation of 1,2-DMCH to *o*-xylene took place without intermediate dehydrogenation products being detected. Isomerization and dehydrogenation did not take place in the absence of hydrogen. The *cis*-to-*trans* isomerization of 1,2-DMCH followed the same pattern as the *o*-xylene hydrogenation rate, passing through a maximum of *trans* isomer formation at 460 K. The result

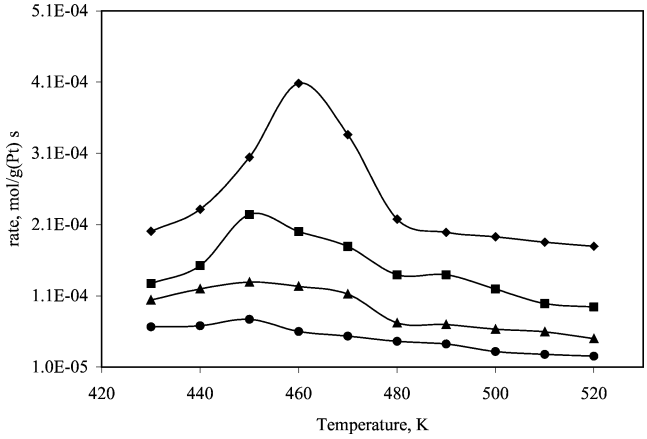

Fig. 2. Temperature dependence of the rate of *o*-xylene hydrogenation over 1 wt% Pt/Al_2O_3–Cl catalyst at different hydrogen concentrations. Conditions: $p_{o\text{-xyl}} = 0.06$ bar; (◆) $p_{H_2} = 0.36$; (■) $p_{H_2} = 0.30$; (▲) $p_{H_2} = 0.24$ bar; (●) $p_{H_2} = 0.19$ bar.

Table 3
Reaction orders with respect to hydrogen in the hydrogenation of *o*-xylene and formation of 1,2-DMCHs over 1 wt% Pt/Al_2O_3–Cl catalyst (conditions: $p_{H_2} = 0.19$–0.36, $p_{o\text{-xyl}} = 0.06$ bar)

T (K)	Order with respect to H_2 in		
	o-Xylene	*cis*-1,2-DMCH[a]	*trans*-1,2-DMCH[a]
430	1.6	1.7	1.3
440	1.8	1.8	1.5
450	2.1	2.2	2.0
460	2.3	2.3	2.5
470	2.7	2.7	2.6
480	2.4	2.6	2.3
490	2.4	2.5	2.3
500	2.7	2.7	2.7
510	2.8	2.7	2.9
520	3.0	2.9	2.9

[a] Formation.

is an indication of the dehydrogenation of *cis*-1,2-DMCH to *o*-xylene, the formation rate of which increased rapidly above 673 K (Fig. 7). Table 4 presents the reaction orders with respect to hydrogen in the formation of *o*-xylene and *trans*-1,2-DMCH as well as the consumption of *cis*-1,2-DMCH. The rate of *trans* isomer formation increased with increasing hydrogen partial pressure, whereas a complex relationship between the hydrogen partial pressure and *cis* isomer consumption was found. At lower temperatures, the rate of *cis* isomer consumption exhibits a positive dependency on the hydrogen partial pressure but is not affected or slightly inhibited by hydrogen above 480 K (Fig. 7a, Table 4). The rate of *o*-xylene formation, on the other hand, is suppressed by hydrogen (Table 4, Fig. 7b). The inhibitory effect of hydrogen on the formation of *o*-xylene decreases with increasing temperature (Fig. 7b, Table 4). This is probably due to the faster desorption of *o*-xylene at higher temperatures, which was confirmed by the *o*-xylene TPD, as mentioned in Section 3.1. The activation energies for the *cis*-to-*trans* isomerization and *o*-xylene formation between 430 and 520 K were 19.7 and 171.2 kJ/mol, respectively. The

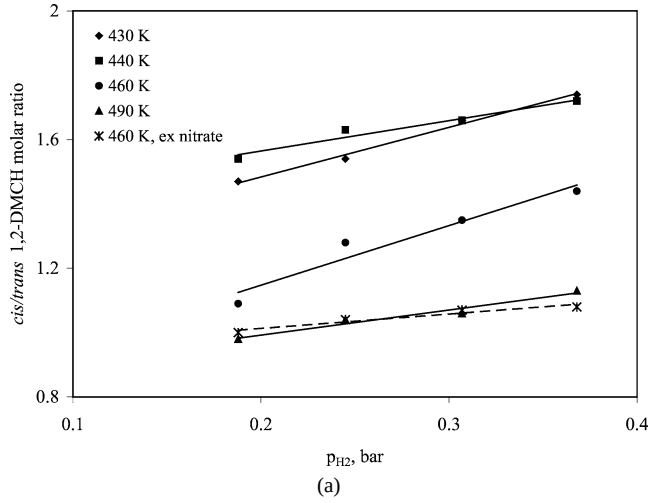

Fig. 3. Dependence of the *cis*-to-*trans* 1,2-DMCH ratio on the concentration of the reactants at different temperatures over 1 wt% Pt/Al_2O_3–Cl catalyst: (a) hydrogen ($p_{o\text{-xyl}} = 0.06$ bar); (b) *o*-xylene ($p_{H_2} = 0.36$ bar).

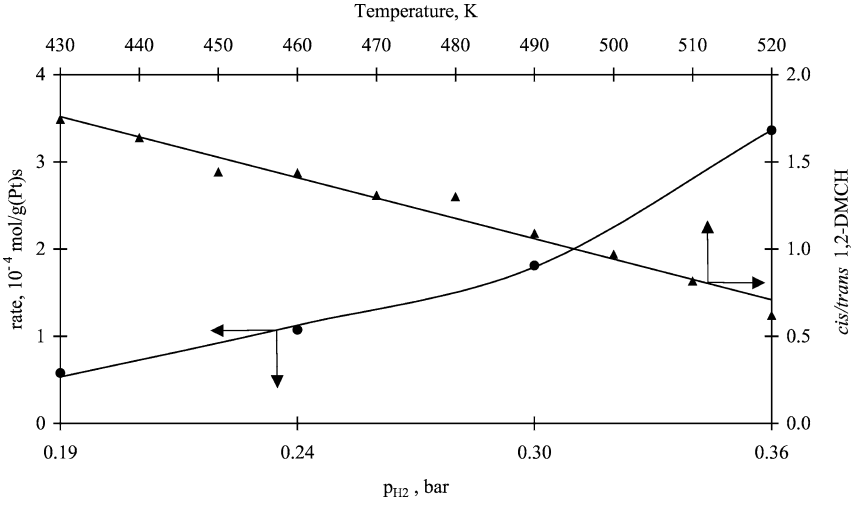

Fig. 4. Dependency of the reaction rate in *o*-xylene hydrogenation and product stereoselectivity on hydrogen concentration and temperature over 1 wt% Pt/Al_2O_3–Cl catalyst: (▲) *cis*-to-*trans* ratio ($p_{H_2} = 0.36$, $p_{o\text{-xyl}} = 0.06$ bar) and (●) *o*-xylene hydrogenation rate ($p_{o\text{-xyl}} = 0.06$ bar, $T = 470$ K).

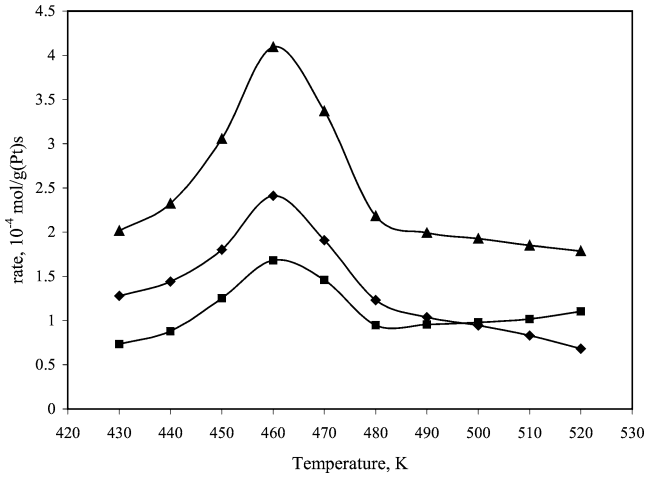

Fig. 5. The rate of *o*-xylene hydrogenation and formation of products at different temperatures over 1 wt% Pt/Al_2O_3–Cl catalyst. Conditions: $p_{H_2} = 0.36$ and $p_{o\text{-xyl}} = 0.06$ bar. (◆) r_{cis}; (■) r_{trans}; (▲) r_{total}.

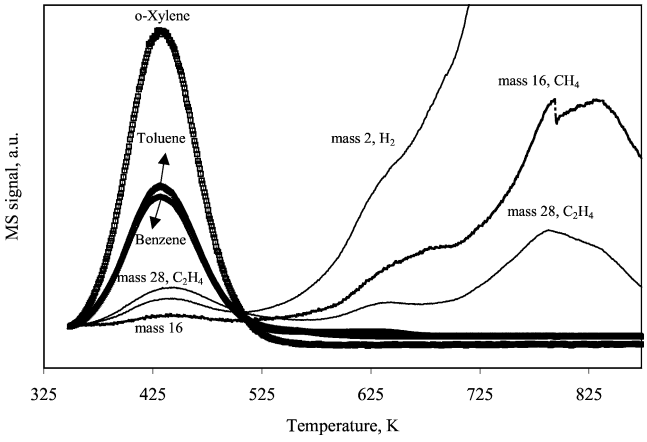

Fig. 6. The TPD pattern of *o*-xylene over 1 wt% Pt/Al_2O_3–Cl catalyst. Carrier gas: Ar.

relatively high apparent activation energy for the dehydrogenation reaction is in accordance with values reported in the literature; one study reported energies of 86–156 kJ/mol for cyclohexane dehydrogenation for alumina-supported Pt, Rh, and Ir catalysts [45]. The activation energies for the *trans* isomer formation was 35.8 and −24.8 kJ/mol at 430–460 and 460–520 K, respectively.

To investigate the effect of the catalyst precursor on the configurational isomerization/dehydrogenation of 1,2-DMCH, the performance of the 1 wt% Pt/Al_2O_3–N catalyst was studied at 460 K. A similar initial rate of *cis*-to-*trans* isomerization was obtained as for the 1 wt% Pt/Al_2O_3–Cl catalyst. However, the catalyst prepared from the nitrate salt underwent strong deactivation in the *cis*-to-*trans* isomerization (Table 5). On the other hand, minor activation with time on stream was observed during dehydrogenation. While chlorine is an inhibitor of *o*-xylene hydrogenation, it acts as a promoter for the configurational isomerization reaction. The dehydrogenation of the 1,2-DMCH to *o*-xylene is not affected by the presence of surface chlorine (Table 5).

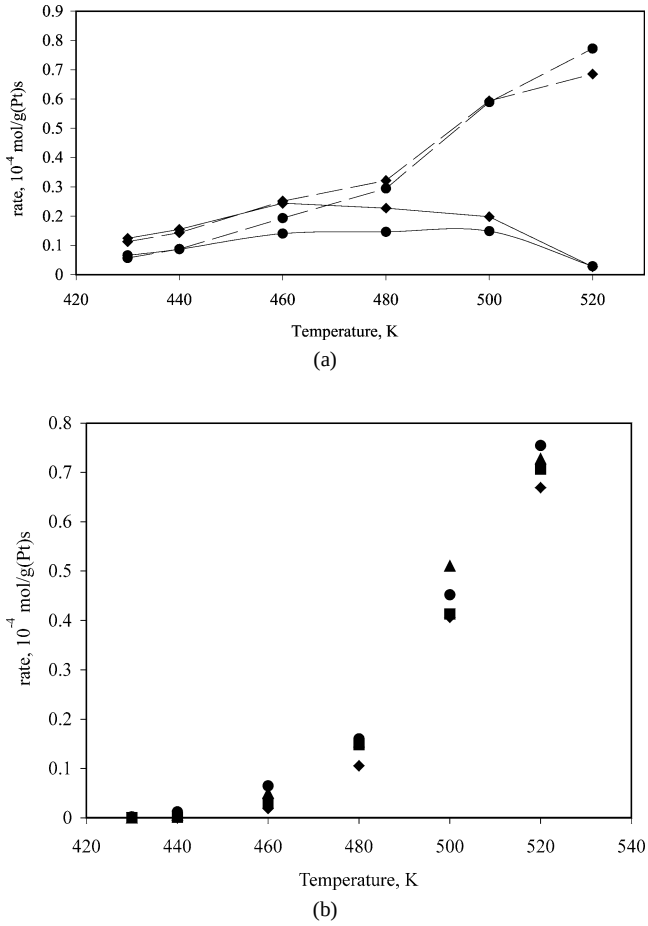

Fig. 7. The *cis–trans*-1,2-DMCH isomerization (a) and 1,2-DMCH dehydrogenation (b) over 1 wt% Pt/Al_2O_3–Cl catalyst. Broken line, *cis*-1,2-DMCH consumption; solid line, *trans*-1,2-DMCH formation. Conditions: $p_{cis\text{-}1,2\text{-DMCH}} = 0.77 \times 10^{-3}$ bar and $p_{trans\text{-}1,2\text{-DMCH}} = 0.14 \times 10^{-3}$ bar. (◆) $p_{H_2} = 0.36$; (■) $p_{H_2} = 0.30$; (▲) $p_{H_2} = 0.24$ bar; (●) $p_{H_2} = 0.19$ bar.

Table 4
Reaction orders with respect to hydrogen in isomerization/dehydrogenation reactions over the 1 wt% Pt/Al_2O_3–Cl catalyst (conditions: $p_{H_2} = 0.19$–0.36 bar, $p_{cis\text{-}1,2\text{-DMCH}} = 0.77 \times 10^{-3}$ bar and $p_{trans\text{-}1,2\text{-DMCH}} = 0.14 \times 10^{-3}$ bar)

T (K)	Orders in H_2 for formation/consumption		
	cis-1,2-DMCH	*trans*-1,2-DMCH	*o*-xylene
430	[a]	[a]	[a]
440	0.7	0.9	[a]
460	0.3	0.8	−1.8
480	0.1	0.6	−0.6
500	0.04	0.4	−0.2
520	−0.2	[a]	−0.2

[a] Low or no conversion for accurate determination.

4. Discussion

4.1. Surface composition

The N_2 physisorption of the freshly prepared catalysts indicated that the incorporation of the platinum into the alu-

Table 5
Behavior of the Pt catalysts in dehydrogenation and isomerization of 1,2-DMCH (conditions: $T = 460$ K, $p_{H_2} = 0.36$ bar, $p_{cis\text{-}1,2\text{-DMCH}} = 0.77 \times 10^{-3}$ bar and $p_{trans\text{-}1,2\text{-DMCH}} = 0.14 \times 10^{-3}$ bar)

Catalyst	Initial rate (10^{-4} mol/(g_{Pt} s))			Rate after 100 min (10^{-4} mol/(g_{Pt} s))		
	r_{cis}	r_{trans}	$r_{o\text{-xyl}}$	r_{cis}	r_{trans}	$r_{o\text{-xyl}}$
1 wt% Pt/Al_2O_3–Cl	0.441	0.439	0.013	0.25	0.24	0.019
1 wt% Pt/Al_2O_3–N	0.354	0.353	0.012	0.055[a]	0.046[a]	0.020

[a] Steady state was not reached.

mina support did not affect the specific surface areas to a great extent, although a decrease in the specific pore volume was observed. The BET surface area and specific pore volume of the support were 219 m^2/g and 0.93 cm^3/g; those of the 1 wt% Pt/Al_2O_3–Cl sample were 217.8 m^2/g and 0.43 cm^3/g, and those of the 4.2 wt% Pt/Al_2O_3–Cl samples were 216.3 m^2/g and 0.62 cm^3/g. Since the presence of surface Cl species had a strong influence on the performance of the catalyst, the compositions of the surface and subsurface were carefully studied by EDXA and XPS (Table 2, Fig. 8). In addition to the high (4.2 wt%) and low (1 wt%) Pt-loading catalysts, a platinum wire and a platinum single crystal (111) were studied as references. The challenges associated with the XPS determination of the states of platinum particles on high surface area alumina surfaces caused by the overlapping of the Al $2p$ and Pt $4f$ XP lines are well known and have been discussed elsewhere [27].

For the low Pt-loaded catalyst, i.e., 1 wt% Pt/Al_2O_3–Cl, the Cl/Al atomic ratio of the samples, which were freshly dried and reduced at different temperatures and determined by EDXA and XPS techniques, were fairly close and were not significantly affected by the reduction temperature (Table 2). However, this was not the case with the 4.2 wt% Pt/Al_2O_3–Cl catalyst, for which both the EDXA and XPS data indicated a decrease in the Cl/Al ratio at increased reduction temperature. The presence of chlorine in the subsurface layers was confirmed, as the sputtered 1 wt% Pt/Al_2O_3–Cl sample still exhibited the same order of magnitude of surface chlorine concentration. The small differences in the Cl/Al ratio obtained by means of the two techniques are probably due to a difference in analyzing depth, XPS being a "surface-sensitive" method and EDXA a technique that has a significantly deeper penetration range (5–10 μm, depending on the density and morphology of the material). Nevertheless, the EDXA indicates that the overall Cl/Al ratio does not change to a great extent after catalyst reduction. Our observations are in good agreement with those reported by Barbier et al. [46] who studied chlorine retention on alumina-supported platinum catalysts and reported a greater chlorine retention with lower Pt loadings; their 0.6 wt% Pt/alumina catalyst retained all the initial chlorine, whereas their 6 wt% Pt/alumina catalyst lost a part of the initial chlorine.

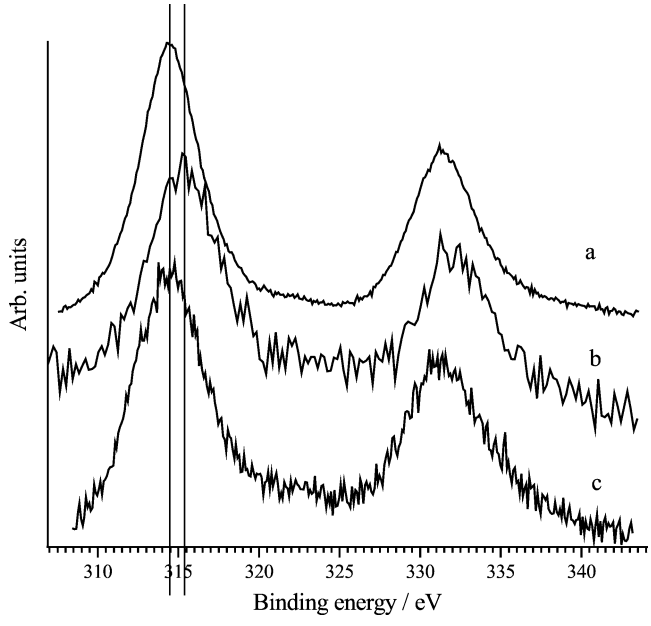

Fig. 8. Pt $4d$ XPS lines. (a) Pt(111), (b) 4.2 wt% Pt/Al_2O_3–Cl freshly dried, and (c) 4.2 wt% Pt/Al_2O_3–Cl reduced at 673 K.

Table 2 lists the Pt $4d_{5/2}$ XPS binding energies (BE) and relates them to those of the platinum wire. The Pt $4d_{5/2}$ BE values of the fresh samples shifted to higher energy levels (315.3 vs 314.3 eV). Hydrogen treatment of the samples at 573 and 673 K restored the binding energies to values "close" to those observed for the Pt(111) and clean platinum wire (Fig. 8, Table 2).

The EDX analysis of the fresh Pt catalysts indicated Cl/Pt ratios of about 3.5, which is another indication that most of the chlorine remains on the catalyst. Reduction of the 1 wt% Pt/Al_2O_3–Cl catalyst did not change the Cl/Pt ratio to a great extent, whereas the Cl/Pt ratio of the 4.2 wt% Pt/Al_2O_3–Cl catalyst decreased by about 25% after catalyst reduction at 673 K. It is interesting that the XPS data indicated an increase in the Cl/Pt surface ratio as a result of higher reduction temperatures (Table 2). This does not agree with the Cl/Al ratios discussed earlier. The characteristic overlapping of the Pt $4f$ and Al $2p$ XP lines and the relatively low signal intensity of the low platinum-containing catalyst (1 wt% Pt/Al_2O_3–Cl) can strongly affect the accuracy of the Pt/Cl ratios. At the same time, the application of the Shirley background [47] to the Pt $4d$ line could introduce additional irregularities due to the shape of the Al_2O_3 background. Hence, the data obtained for 4.2 wt% Pt/Al_2O_3–Cl is more accurate and will be discussed below.

Although the XPS data clearly indicate the existence of surface Cl species, the shifts in the Pt BEs and the conflicting Pt/Al and Pt/Cl ratios require more attention. The reasons for the observed shift in the Pt BEs and the unexpected Pt/Al and Pt/Cl ratios is probably due to the effect of the chlorine coordination to the platinum as well as to the effect of the particle size of the platinum on the accuracy of the XPS analysis.

Table 2 lists the results of the particle size calculations by XPS. They indicate that the particle size of the platinum

of the freshly dried catalysts is in the range of 0.7–0.8 nm in diameter. On the freshly dried catalyst, chlorine is associated with the platinum particles on the platinum–alumina interface and will modify the electrical properties of this interface. The acidic sites of the support will probably lead to additional electron withdrawal. Joyner et al. [48] demonstrated that the electronic perturbation at the Pd interface of the support is in a range of no more than 0.5 nm into the particle. Assuming that the same magnitude of interaction is also valid for platinum, the surface platinum particles (0.7–0.8 nm) of the freshly dried catalyst with a high platinum loading (4.2 wt% Pt) will be affected strongly by the environment, i.e., by the electronegative chlorine atoms. The reduction of the catalyst at 673 K results in the formation of relatively larger platinum particles (ca. 1.6 nm); hence, a considerable portion of the platinum particle will not be affected by the acidity of the support or by chlorine. The platinum lattice constant (a) is about 0.39 nm [49]; assuming cubic geometry, it is reasonable that for the high-loaded Pt–Al_2O_3 catalyst, only the first platinum layer will expect to be affected by the environment in terms of electron transfer. Such e^- transfer from the metal–support interface to the electron acceptor entities results in a net positive charge that is de-localized on the particle surface, while a zero charge is established inside the particle. Thus, for the Pt catalyst with larger particles, a BE value closer to that observed for metallic platinum is expected. This explains the shifts in the $4d_{5/2}$ Pt BEs at different reduction temperatures because the platinum particles grow with increasing reduction temperature. Another manifestation of the chlorine effect on the Pt $4d_{5/2}$ BE can be seen from the XPS analysis of the ex-nitrate catalyst (Table 2), where the freshly dried sample and the sample reduced at 673 K exhibited BE values similar to those of the platinum wire (314.9 and 314.2 vs 314.3 eV). Furthermore, chlorine on the freshly dried sample is directly associated with a highly dispersed adsorbed platinum–chlorine complex (Pt diameter of ca. 0.7 nm). As well as inducing sintering, catalyst reduction can result in the migration of chlorine from the platinum Cl complex to the support and platinum–support interfaces. This in turn can lower the withdrawal of the electrons from the platinum particle; consequently, a less positively charged Pt species is detected by XPS (giving a BE closer to that of metallic platinum). For the Pt/Al_2O_3–Cl systems with a relatively low platinum content, it is, unfortunately, impossible to deconvolute the peaks related to the $PtCl_x$ species. The Pt 4d line from $PtCl_2$ is at about 317 eV and is too wide for meaningful deconvolution to be applied. The XP signal also depends on the particle size and becomes weaker with increasing depth of penetration. This explains the observed increase in Cl/Pt and the decrease in the Pt/Al ratio after reduction of the catalyst (Table 2). A weak signal, induced by an increase in the particle size, results in an erroneous quantitative measurement of the total content of platinum (less Pt is detected).

4.1.1. Source of chlorine

The chlorine originates from the dissociation of hexachloroplatinic acid. The EDX data indicate Pt/Cl ratios of about 3.5 in the freshly dried samples (Table 2). These values are close to those reported by Berdala et al. [50]; in their study, the EXAFS measurements demonstrated that the precursor interacts strongly with the support on the dried ex-H_2PtCl_6/Al_2O_3 catalyst, leading to the formation of predominantly $PtCl_4O_2$ species.

4.2. o-Xylene hydrogenation

The results at different temperatures indicate the presence of a maximum in hydrogenation activity at all the H_2/o-xylene ratios investigated (Fig. 2). A thermodynamic calculation of the gas composition at the operation temperatures indicate that the experimental data are not close to equilibrium; therefore, the decrease in the rate of hydrogenation above 460 K can be attributed solely to kinetic effects. The temperature dependence of TON was explained as a combined effect of an increase in the hydrogenation rate on the catalyst surface and the accompanying decrease in the concentration of reactive aromatic species on the surface (no data reported), which ultimately results in the formation of T_{max} [16,18]. Such a decrease in the surface coverage of xylene is in good agreement with our o-xylene TPD experiment (Fig. 6) in which the maximum peak in the o-xylene desorption was very close to the temperature of the maximum activity in o-xylene hydrogenation. The H_2 TPD patterns indicated the presence of surface hydrogen from 298 to 873 K. Therefore, the decreased hydrogenation activity at higher temperatures (above 460 K) was not attributed to the decreased hydrogen coverage. The catalyst prepared from the platinum nitrate salt exhibited a higher hydrogenation activity than the 1 wt% Pt/Al_2O_3–Cl catalyst. As mentioned in Section 4.1.1, the chlorine remains on the surface of the 1 wt% Pt/Al_2O_3–Cl catalyst, even after reduction at 673 K, and the lower hydrogenation activity of the 1 wt% Pt/Al_2O_3–Cl is probably due to the negative impact of chlorine, which will be discussed latter.

The TON (Table 1), determined from the number of o-xylene molecules hydrogenated per surface platinum atoms (determined from H_2 chemisorption measurements), indicated a slight decrease in TON due to the larger platinum particles (i.e., compared to the catalysts prepared with the same salt and with higher Pt loadings of 2.7 and 4.2 wt%). However, the TON values are too close to enable a conclusion about the structure sensitivity of the o-xylene hydrogenation. The structure sensitivity of the xylene hydrogenation was reported for platinum and ruthenium systems [21,24], whereas no effect of dispersity on the activity of palladium was observed [10]. The hydrogenation activity was found to be a function of the reduction temperature of the catalyst (Table 1). The higher activity as a result of the higher reduction temperature of the catalyst is correlated almost linearly to the amount of hydrogen desorbed from the

exposed surface of the platinum (Table 1). The increase in the hydrogen desorption due to an increase in the reduction temperature of the catalyst is believed to be due to the redistribution of residual chlorine on the catalyst surface. The electronic effects, induced by the presence of surface chlorine and its location (coordination to platinum or on alumina in the vicinity of the Pt particles), determine the hydrogen adsorption but not the relatively small changes in the particle size. Such a dependence on the reduction temperature was reported for hydrogenation of xylene and monoalkyl benzenes over platinum [22,51].

The *cis* stereoisomer is the kinetically favored product, at the expense of the thermodynamically favored *trans* isomer (Fig. 2). The *o*-xylene adsorbs with the aromatic ring parallel to the surface [52,53]. To relieve the steric repulsion, the two methyl groups should be oriented away from the surface. Under such conditions, a thermodynamically less stable *cis* isomer forms, i.e., the kinetically favored product. Our data indicate a decrease in the *cis*-to-*trans* ratio from 1.7 (at 420 K) to 0.6 (at 520 K). The higher selectivity to the formation of the *trans* isomer at higher temperatures have been discussed by several scientists. Siegel et al. [54] in the liquid-phase hydrogenation reactions suggested that the cycloalkenes, formed as a result of the *cis* addition of four hydrogen atoms to the xylene molecules, are desorbed from the surface and re-adsorbed; after that hydrogenation of the double bond to form the *trans* isomer takes place. However, the *cis*-to-*trans* ratio of unity and lower is often observed; this suggests that almost half of the tetra-hydrogenated molecules desorb and re-adsorb. Keane et al. [16,18] explained the phenomenon by considering the decrease in the surface concentration of aromatics at higher temperatures and the relief of the geometrical constraints. The authors proposed that weaker surface interactions and a decrease in surface occupation by aromatic with increasing temperature enable a rearrangement of the atoms not directly involved in the binding process and, consequently, an increase in the proportion of the *trans* product. The increase in the selectivity toward the formation of the *trans* isomer as a result of higher temperature and an increase in metal dispersion has often been explained by a rollover mechanism, proposed originally by Inuone et al. [30]. The model provides a good description of the exchange of hydrogen atoms on both sides of the cyclopentane molecule (over Pd catalysts). The same model has been applied to the stereoselectivity of *o*-xylene hydrogenation [10–15,21–24] as the last double bond to be hydrogenated isomerizes before the rollover step. The addition of more hydrogen results in the formation of the *trans* isomer. Scheme 1a represents the rollover mechanism, according to which 1,2-dimethylcyclohexene (1,2-DMCHe) isomerizes to 2,3-dimethylcyclohexene (2,3-DMCHe), and the latter rolls over and provides the condition for the formation of the *trans* isomer by hydrogenation of the double bond. According to this scheme, a desorption and re-adsorption of the 2,3-DMCHe from the other side of the plane, in addition to rollover, are also possible.

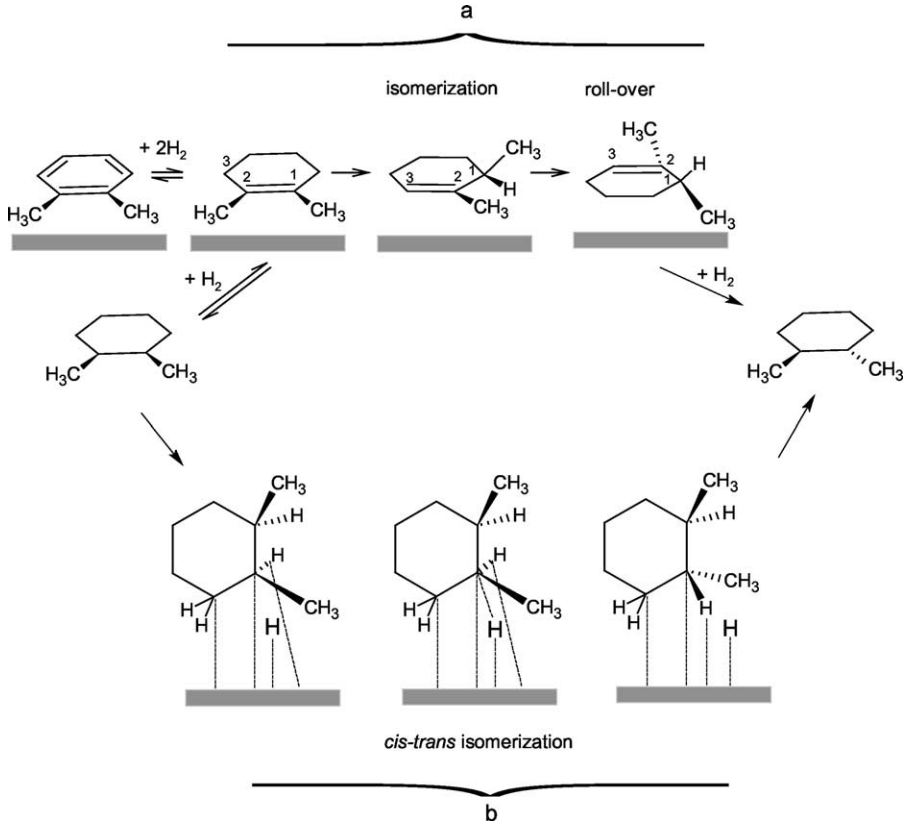

Scheme 1. The reaction paths for *o*-xylene hydrogenation and product stereoselectivity.

As shown in Table 1 for the 1 wt% Pt/Al_2O_3–Cl catalyst, the higher the rate of *o*-xylene hydrogenation, the lower the selectivity toward formation of the *trans* isomer, at the given temperature and concentration of reactants (the lower rate of isomerization of 1,2-DMCHe to 2,3-DMCHe and its further rollover). The selectivity to *trans* isomer formation also decreases with increasing hydrogen concentration (Fig. 3), which results in a higher reaction rate and, consequently, a decrease in selectivity to the *trans* isomer formation. The relative rates of hydrogenation and DMCHe isomerization/rollover are among the more important factors in determining the stereoselectivity. The results of the experiments on varying the *o*-xylene concentration indicated a slight decrease in the *cis*-to-*trans* ratio (0.1–0.2) when the *o*-xylene partial pressure decreases (Fig. 3b). This may indicate that the rate of *trans* isomer formation will increase at higher conversion levels (dependence of product selectivity on the conversion level). In their study of *o*-xylene hydrogenation over Ru catalysts, Viniegra et al. [21] observed a lower selectivity to the formation of the *trans* isomer as a result of lower conversion levels, induced by time-on-stream catalyst deactivation. Similarly, different catalyst reduction temperatures strongly affect the selectivity by enhancing the hydrogenation rate (Table 1).

In contrast to the 1 wt% Pt/Al_2O_3–Cl catalyst, the 1 wt% Pt/Al_2O_3–N catalyst exhibits a higher hydrogenation activity and simultaneously a higher selectivity to the formation of *trans*-1,2-DMCH (Table 1, Fig. 3). The effect of hydrogen partial pressure on the *cis*-to-*trans* ratio was less pronounced for the ex-nitrate catalyst compared to the ex-chloroplatinic acid catalyst (Fig. 3a). These differences in the performance of these two catalysts with similar platinum particle sizes is probably due to the influence of the chlorine anions on the catalyst surface (see Section 4.2.2).

4.2.1. Descriptive kinetics of stereoselectivity

Scheme 2 represents the kinetics of *cis*- and *trans*-1,2-DMCH stereoselectivity, where C, T, and A represent *cis*-1,2-DMCH, *trans*-1,2-DMCH, and *o*-xylene, respectively. The sequential addition of hydrogen was considered. For example, AH_2 and AH_4 represent surface intermediate complexes, which retain their aromatic character. The nature of these intermediates with respect to the thermodynamics has been discussed in detail [14,55]. AH_4 is the precursor of the adsorbed intermediate O, which can undergo hydrogenation to *cis*-1,2-DMCH (step 4). Step 5 in Scheme 2 is assigned to the isomerization of 1,2-DMCHe and the rollover of the intermediate 1,3-DMCHe. The dependence on stereoselectivity results from this mechanism, assuming that step 4 is irreversible,

$$\frac{r_{cis}}{r_{trans}} = k_4 \frac{k_{-5} + k_6 P_{H_2}}{k_5 k_6}, \tag{1}$$

where k_i is the rate constant of the given step. The decrease in selectivity to the *trans* isomer with increasing hydrogen concentration clearly follows from Eq. (1), as was shown by the experimental data. However, Eq. (1) does not show the dependence of stereoselectivity on the partial pressure of *o*-xylene. On the other hand, the experimental data indicated that the *cis:trans* ratio depends to a small extent on the partial pressure of *o*-xylene. The derivation of Eq. (1) is based on a noncompetitive adsorption of reactants, which is probably an oversimplification, assuming competitive adsorption may help to describe the dependence of stereoselectivity on the *o*-xylene concentration. Complete kinetic modeling will be the subject of a separate study.

4.2.2. Effect of chlorine on o-xylene hydrogenation/stereoselectivity

Aromatics are believed to adsorb flat on the surface of group VIII metals via π bonding, which involves electron transfer from the aromatic ring to the unoccupied *d*-metal orbitals. A back-donation of the electron from the metal to the π^* anti-bonding orbital of the aromatic molecule follows. However, adsorption depends to a large extent on the local density of the metal atom. Both the ex-chloroplatinic acid and ex-nitrate catalysts have small metal particles in the range of about 1 nm (Table 1). This results in a decrease in *d*-shell occupation and in the density of states at the Fermi level [56]. This decrease in electron occupation in the valence bond results in a higher binding energy of species such as *o*-xylene, which behave like Lewis base species. As discussed in Section 4.1, additional electron withdrawal, induced by the chlorine anions in the support–platinum interface, results in a further decrease in the occupation of the *d*-shell and, hence, increases the binding energy of the

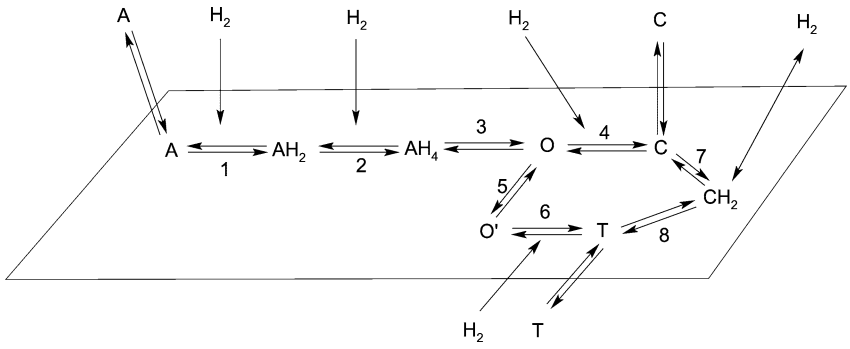

Scheme 2. Descriptive kinetics of *o*-xylene hydrogenation.

adsorbed species. Our XPS data indicate the presence of positively charged Pt particles (Table 2, BEs). The NMR of adsorbed ^{129}Xe and XPS [57,58] has also proven the presence of positively adsorbed Pt species ($Pt^{\delta+}$). Thus, adsorption of xylene, an electron donor, is expected to be stronger on the electron-deficient platinum sites. On the other hand, xylene adsorption takes place readily on the surfaces of noble metals (in the temperature range studied), as proven by the xylene TPD experiments (Fig. 6). Hence, an increase in the adsorption strength might have a negative impact on the hydrogenation of the aromatic ring. Moreover, decreased electron transfer from $Pt^{\delta+}$ to the π^* anti-bonding orbital of the aromatic ring of chemisorbed xylene diminishes the activity of the aromatic ring and, consequently, decreases the hydrogenation rate. This negative effect of chlorine was also reported in the hydrogenation of phenol and styrene: the hydrogenation rates were lower over the palladium catalysts prepared from chlorided salts [59,60].

The selectivity toward the formation of a *trans* isomer decreases with decreasing platinum particle size (Table 1), due to the impact of the precursor on the properties of the final catalyst. As discussed above, the electric properties of small metal particles are strongly affected by the environment (and, in our case, by the presence of electronegative chlorine). When the particles are larger, the portion of surface atoms with different coordination numbers varies. The larger the particle, the less it is influenced by the environment and eventually exhibits bulk metallic behavior (or less positively charged platinum particles, as shown by XPS analysis). Hence, the ex-chloroplatinic acid catalyst with larger Pt particles exhibits stereoselectivity, more similar to that of the Cl-free catalyst (i.e., higher selectivity toward *trans* isomer formation (Table 1). For the platinum catalysts with larger particles, the increase in selectivity to the formation of a *trans* isomer may be due not only to the dependence of selectivity on the conversion levels but also to the weaker effect of the residual chlorine. In their study of *o*-xylene hydrogenation over a Pt/Al_2O_3 catalyst, Saymeh et al. [23] concluded that the selectivity to the *trans* isomer increases with greater dispersion. They explained their observation in terms of the rollover mechanism and argued that a larger number of sites is required for the rollover mechanism to be more effective. The surface available to the reactants is certainly of crucial importance in catalytic reactions. However, those authors studied catalysts with relatively low levels of dispersion (13–50%), whereas our catalysts have rather high levels of dispersions and large metallic surfaces for the adsorption of the reactant (Table 1). According to the rollover mechanism (Scheme 1a), it might be assumed that a longer residence time of the intermediates favors the formation of the *trans* isomer. An increase in the strength of adsorption, i.e., a longer time on the surface, does not necessarily mean greater likelihood of the formation of the *trans* isomer; indeed, as observed in the present study, the ex-nitrate catalyst exhibits a higher selectivity toward the formation of the *trans* isomer.

4.3. Dehydrogenation and configurational isomerization

The *o*-xylene hydrogenation experiments indicate an increase in the reaction order with respect to hydrogen as the temperature of the operation increases. Such high reaction orders (up to 3) may indicate the existence of hydrogen-deficient surface species. They may also indicate the competitive dehydrogenation of the products, leading to high orders with respect to hydrogen. In their study of the hydrogenation of benzene and toluene, Vannice et al. [9,61] proposed a concurrent surface dehydrogenation reaction involving the aromatic reactant and resulting in the formation of hydrogen-deficient surface species.

The concurrent dehydrogenation and *cis*- to *trans*-1,2-DMCH epimerization reactions were found to take place at high rates over alumina-supported Pt catalysts (Figs. 7a and 7b). The presence of hydrogen was essential for the dehydrogenation and isomerization reactions: when the hydrogen flow was halted (balanced by argon), the reactions deceased immediately. By re-introducing the hydrogen, about 75% of the activity at steady state was restored (over the 1 wt% Pt/Al_2O_3–Cl catalyst). In their study of configurational isomerization of dimethylcyclohexane over an alumina-supported platinum catalyst, Bragin et al. [62] found a similar restoration of the activity. The effect of hydrogen on the reaction rate indicates that hydrogen plays a role not only in the removal of carbon deposition but also, crucially, in the reaction mechanism.

The *cis*-to-*trans* configurational isomerization passes through a maximum at 460 K. Above 460 K, aromatization is the dominant reaction, and the *cis*-1,2-DMCH is dehydrogenated to *o*-xylene (Figs. 7a and 7b). This is in fairly good agreement with *o*-xylene TPD experiments, in which *o*-xylene desorbed almost completely at temperatures exceeding 440 K (Fig. 6). At lower temperatures (below 440 K), the produced xylene is apparently strongly adsorbed on the surface and inhibits the dehydrogenation of 1,2-DMCH. There have been few studies on DMCH adsorption and dehydrogenation on platinum surfaces [37,38]. However, the dehydrogenation of cyclohexane has been the subject of many studies. Cyclohexane was reported to undergo dehydrogenation readily on Pt(111) [53]. At low temperatures only a small amount of the formed benzene is desorbed to the gas phase; its desorption is intensified at temperatures exceeding 480 K [63]. The presence of aromatics has also inhibited the cyclohexane dehydrogenation [29,45].

4.3.1. Descriptive kinetics of isomerization and dehydrogenation of 1,2-DMCH

The dehydrogenation of naphthenes probably follow a sequential dehydrogenation path. Cyclohexene was detected on the Pt(111) surface after cyclohexane dehydrogenation [64]. However, there is no proof that cycloalyl or cyclohexadiene are present on platinum surfaces. The dehydrogenation of *cis*-1,2-DMCH to *o*-xylene is represented qualitatively by the stepwise abstraction of the hydrogen

molecules (Scheme 2), with the first step determining the rate. Further, dehydrogenation of adsorbed 1,2-DMCHe takes place rapidly. Moreover, it can further undergo isomerization and rollover. As mentioned in Section 4.2.1, the adsorbed reactants compete with each other. Therefore, competitive adsorption is represented below,

$$r = \frac{k_{-4} K_C P_C}{(1 + K_C P_C + K_A P_A + K_{H_2} P_{H_2})^2}, \quad (2)$$

where K_C and K_H denote the adsorption constant for *cis*-1,2-DMCH and hydrogen adsorption coefficient, respectively. At low temperatures, the value of K_H is high; therefore, the contribution of $K_{H_2} P_{H_2}$ is significant, leading to a reaction order for hydrogen of about -2. At the same time, desorption of hydrogen predominates at higher temperatures and dependence on the hydrogen pressure is less pronounced (Table 4).

Reflection absorption IR spectroscopy (RAIRS) and spectroscopic studies of high-resolution electron energy loss [65,66] revealed that cyclohexane is adsorbed with the plane parallel to the surface and very likely in a chair conformation, with three axial hydrogen atoms directed toward the surface, forming hydrogen bonds. Cyclohexene is believed to adsorb on the Pt(111) surface as di-σ bonded [67,68], whereas cyclohexadiene induces a surface bond of the quadra-σ type (with sp^3 hybridization of the involved carbons) [68,69]. From the above-mentioned adsorption data, the isomerization of 1,2-DMCH can be described as a dissociative mechanism (S_N2) (Scheme 1b). According to this mechanism, *cis*-1,2-DMCH adsorbs parallel to the surface with hydrogen atoms forming H bondings. As was also confirmed by the experimental data, the presence of surface hydrogen is essential in this case. The coordination of the adsorbed hydrogen to the ring and its further exchange to the ring results in the formation of *trans*-1,2-DMCH (Scheme 1b). Isomerization of *cis*-to-*trans* by means of the S_N2 mechanism is represented in Scheme 2. To derivate the kinetic equation of isomerization, it is assumed that hydrogen does not compete with organic molecules for surface sites since the reaction probably takes place on the alumina–platinum interfaces. The rate of *cis*-1,2-DMCH isomerization, at low conversion levels, is expressed as

$$r = \frac{k_7 k_8 K_C P_{H_2} P_C}{(k_{-7} + k_8)(1 + K_C P_C + k_7 K_C P_{H_2} P_C)}. \quad (3)$$

At low temperatures, the reaction order with respect to H_2 for the consumption of *cis*-1,2 DMCH and *trans*-1,2-DMCH formation is close to unity and decreases with increasing temperature. As the temperature increases, the impact of $k_7 K_C P_{H_2} P_C$ in the denominator becomes stronger, resulting in a lower reaction order with respect to hydrogen.

4.3.2. Effect of chlorine on dehydrogenation and configurational isomerization

As in the case of *o*-xylene hydrogenation, the ex-platinic acid and ex-nitrate catalysts behaved differently. The ex-chloroplatinic acid catalyst exhibited higher activity in the isomerization, while both catalysts exhibited similar activity in 1,2-DMCH aromatization. The 1 wt% Pt/Al_2O_3–N catalyst underwent strong deactivation in *cis*-to-*trans*-1,2-DMCH isomerization, even though it remained active during dehydrogenation (Table 5). Over Pt/Al_2O_3, two sites are occupied for these reactions. The metallic component is responsible for the hydrogenation–dehydrogenation activity, whereas the platinum–alumina interfaces are active in the isomerization reaction, which is stronger with increasing acidity of the support (or local site). The presence of surface chlorine was reported to enhance the dehydrogenation of cyclohexane over Pt and Pt–Re catalysts [45]. The authors reported that 3% chlorine is optimum for increasing the activity of dehydrogenation. This was attributed to increased hydrogen spillover. In the present study, the activity of the Cl-containing and the Cl-free catalysts in 1,2-DMCH dehydrogenation was the same. Here, no additional chlorine was added to the catalyst; and, thus, the surface chlorine originated solely from the chlorine anions of hexachloroplatinic acid. Although our H_2 TPD data did not reveal greater spillover of hydrogen in the presence of surface Cl species, the acidity of the neighboring OH^- groups certainly increased. This may result in a greater local hydrogen spillover. The alumina-supported platinum catalyst, prepared from chloroplatinic acid, is more active than the corresponding catalyst prepared from the platinum acetylacetonate precursor [70].

1,2-DMCH isomerization was accompanied by deactivation, which was greater in the case of the chlorine-free catalyst. Deactivation due to coke formation is a complex process and is associated with the majority of catalyzed organic reactions. In their study of coke deposition on a bifunctional Pt/Al_2O_3–Cl catalyst, Barbier et al. [71] demonstrated that the carbon coverage of the metal increases during the first few minutes of the reaction and remains constant, while further coke accumulation proceeds by deposition on the support. The presence of chlorine on the surface of the 1 wt% Pt/Al_2O_3–Cl catalyst can increase the acidity of the catalyst and induce greater spillover of local hydrogen, thus leading to the removal of the coke precursors from the alumina–Pt interface. In contrast, the coke buildup on the interface of metal–support of the ex-nitrate catalyst blocks the sites for *cis*-to-*trans* isomerization.

5. Conclusion

The gas-phase hydrogenation of *o*-xylene was studied from 430 to 520 K. The *o*-xylene hydrogenation passes through a reversible maximum at 460 K. The *cis*-1,2-DMCH is the kinetically favored product, whereas selectivity to the formation of the thermodynamically favored *trans* product increases with increasing operation temperature. The stereoselectivity depends on the conversion levels, the reactant concentration, and the nature of the catalyst precursor. Chlorine remains on the catalyst surface even after reduction at

673 K and inhibits hydrogenation. Simultaneous aromatization and epimerization of the products take place, and the presence of hydrogen is essential for these reactions. The residual chlorine did not affect the aromatization reaction to a great extent. However, chlorine promotes the *cis*-to-*trans* configurational isomerization reaction. The *o*-xylene hydrogenation reaction probably occurs by the sequential addition of hydrogen in that most if not all of the *trans*-1,2-dimethylcycloalkane arises via the isomerization of the 1,2- to the 2,3-dimethylcycloalkene followed by the rollover of the latter or desorption and re-adsorption on the other side of the ring. Although the stereoselectively is affected mostly by the ratio of the rates of hydrogenation and 1,2-DMCHe isomerization, some of the *cis*-1,2-dimethylcycloalkane is probably converted directly to the *trans* saturated product via configurational isomerization (Scheme 1).

Acknowledgments

The financial support from the Academy of Finland is gratefully acknowledged. This work is a part of the activities at the Åbo Akademi Process Chemistry Group within the Finnish Center of Excellence Programme (2000–2005) by the Academy of Finland.

References

[1] S. Toppinen, T.-K. Rantakylä, T. Salmi, J. Aittamaa, Ind. Eng. Chem. Res. 35 (1996) 4424.
[2] A. Stanislaus, B.H. Cooper, Catal. Rev. Sci. Eng. 36 (1994) 75.
[3] M.V. Rahaman, M.A. Vannice, J. Catal. 127 (1991) 251.
[4] S. Smeds, D. Murzin, T. Salmi, Appl. Catal. A 125 (1995) 271.
[5] S. Smeds, T. Salmi, D. Murzin, Appl. Catal. A 185 (1999) 131.
[6] S. Smeds, T. Salmi, D. Murzin, Appl. Catal. A 201 (2000) 55.
[7] S.D. Lin, M.A. Vannice, J. Catal. 143 (1993) 359.
[8] S.D. Lin, M.A. Vannice, J. Catal. 143 (1993) 554.
[9] S.D. Lin, M.A. Vannice, J. Catal. 143 (1993) 563.
[10] M. Viniegra, G. Córdoba, R. Gómez, J. Mol. Catal. 58 (1990) 107.
[11] G. Cordoba, J.L.G. Fierro, A. López-Goana, N. Martin, M. Viniegra, J. Mol. Catal. A: Chem. 96 (1995) 155.
[12] N. Martin, G. Córdoba, A. López-Gaona, M. Viniegra, React. Kinet. Catal. Lett. 44 (1991) 381.
[13] S. Smeds, T. Salmi, D. Murzin, Appl. Catal. A 145 (1996) 253.
[14] S. Smeds, D. Murzin, T. Salmi, Appl. Catal. A 141 (1996) 207.
[15] S. Smeds, T. Salmi, D. Murzin, Appl. Catal. A 150 (1997) 115.
[16] M.A. Keane, J. Catal. 347 (1997) 166.
[17] M.A. Keane, P.M. Patterson, Ind. Eng. Chem. Res. 38 (1999) 1295.
[18] M.A. Keane, P.M. Patterson, J. Chem. Soc. Faraday Trans. 92 (1996) 1413.
[19] B. Coughan, M.A. Keane, Zeolites 11 (1991) 12.
[20] B. Coughan, M.A. Keane, Catal. Lett. 5 (1990) 101.
[21] M. Viniegra, N. Martin, A. López-Gaona, G. Córdoba, React. Kinet. Catal. Lett. 49 (1993) 353.
[22] M.A. Aramendía, V. Borau, C. Jiménez, J.M. Marinas, F. Rodero, M.E. Sempre, React. Kinet. Catal. Lett. 46 (1992) 305.
[23] R.A. Saymeh, H.M. Asfour, Orient. J. Chem. 16 (2000) 67.
[24] R.A. Saymeh, H.M. Asfour, W.A. Tuaimen, Asian J. Chem. 9 (1997) 350.
[25] R.A. Saymeh, H.M. Asfour, W.A. Tuaimen, Indian J. Chem. B 36 (1997) 799.
[26] A. Kalantar Neyestanaki, P. Mäki-Arvela, H. Backman, H. Karhu, T. Salmi, J. Väyrynen, D.Yu. Murzin, J. Mol. Catal. A: Chem. 193 (2003) 237.
[27] H. Karhu, A. Kalantar, I.J. Väyrynen, T. Salmi, D.Yu. Murzin, Appl. Catal. A, in press.
[28] S.L. Kiperman, D. Shopov, A. Andreev, N. Zlotina, B. Gudkov, Comm. Dept. Chem. Bulg. Acad. Sci. 4 (1971) 237.
[29] J.E. Geramin, R. Maurel, J. Burgeois, R. Sinn, J. Chim. Phys. 60 (1963) 1219.
[30] Y. Inuone, J.M. Herrmann, H. Schmidt, R.L. Burwell, J.B. Butt, J.B. Cohen, J. Catal. 53 (1978) 401.
[31] O.B. Belskaya, N.M. Ostrovskii, Yu.K. Demanov, React. Kinet. Catal. Lett. 60 (1997) 119.
[32] D.W. Blakely, G.A. Somorjai, J. Catal. 42 (1976) 181.
[33] J.L. Gland, K. Baron, G.A. Somorjai, J. Catal. 36 (1975) 305.
[34] J.H. Sinfelt, Y.L. Lam, J. Catal. 42 (1976) 319.
[35] R.W. Maatman, P. Mahaffy, P. Hoekstra, C. Addink, J. Catal. 23 (1971) 105.
[36] A.N. Mitrofanova, V.S. Boronin, O.M. Poltorak, Zh. Fiz. Khim. 46 (1972) 32.
[37] D. Shopov, A. Andreev, Neftekhim 6 (1966) 539.
[38] L. Petrov, D. Shopov, Izv. Otd. Khim. Nauki Bulg. Akad. Nauk 2 (1969) 903.
[39] F.G. Ciapetta, D.N. Wallace, Catal. Rev. Sci. Eng. 5 (1971) 63.
[40] S.M. Davis, J. Catal. 122 (1990) 240.
[41] R. Hudges, Deactivation of Catalysts, Academic Press, London, 1984.
[42] P.G. Menon, Chem. Rev. 94 (1994) 1021.
[43] R. Kramer, M. Andre, J. Catal. 58 (1979) 287.
[44] C.A. Brown, J. Am. Chem. Soc. 91 (1969) 5901.
[45] L.I. Ali, A.-G. Ali, S.M. Abou-Fotouh, A.K. Aboul-Gheit, Appl. Catal. A 177 (1999) 99.
[46] J. Barbier, D. Bahloul, P. Marecot, J. Catal. 137 (1999) 377.
[47] D.A. Shirley, Phys. Rev. B 5 (1972) 4709.
[48] R.W. Joyner, J.B. Pendry, D.K. Saldin, S.R. Tennison, Surf. Sci. 138 (1984) 84.
[49] CRC Handbook of Chemistry and Physics, 75th ed., CRC Press Inc., Boca Raton, FL, 1994.
[50] J. Berdala, E. Freund, J. Lynch, J. Phys. 47 (1986) 269.
[51] M.A. Aramandía, V. Borau, C. Jimenéz, J.M. Marinas, F. Rodero, M.E. Sempre, Bull. Chem. Soc. Jpn. 63 (1990) 1275.
[52] J.W. Peck, B.E. Koel, J. Am. Chem. Soc. 118 (1996) 2708.
[53] B.E. Koel, D.A. Blank, E.A. Carter, J. Mol. Catal. 131 (1998) 39.
[54] S. Siegel, G.V. Smith, B. Dmuchovsky, D. Dubbel, W. Halpern, J. Am. Chem. Soc. 84 (1962) 3136.
[55] S. Smeds, T. Salmi, D. Murzin, React. Kinet. Catal. Lett. 63 (1998) 47.
[56] R.C. Baetzold, J. Phys. Chem. 82 (1978) 738.
[57] S.V. Filimonova, V.M. Mastikin, M.D. Smolikov, A.S. Belyi, V.K. Duplyakin, React. Kinet. Catal. Lett. 48 (1992) 209.
[58] R. Bouwman, P. Biloen, J. Catal. 48 (1977) 209.
[59] N. Mahata, V. Vishwanathan, J. Catal. 196 (2000) 262.
[60] J. Sepuldeva, N. Figoli, React. Kinet. Catal. Lett. 53 (1994) 155.
[61] P. Chou, M.A. Vannice, J. Catal. 107 (1987) 140.
[62] O.V. Bragin, V.G. Tovmacian, D.B. Furman, A.L. Liberman, Isv. Akad. Nauk USSR Ser. Khim. 12 (1976) 2718.
[63] C. Xu, Y.-L. Tsai, B.E. Koel, J. Phys. Chem. 98 (1994) 585.
[64] D.P. Land, W. Erley, H. Ibach, Surf. Sci. 289 (1993) 237.
[65] M.A. Chesters, P. Gardner, Spectrochim. Acta A 46 (1990) 1011.
[66] J.E. Demuth, H. Ibach, H. Lehwald, Phys. Rev. Lett. 40 (1978) 1044.
[67] C. Xu, B.E. Koel, Surf. Sci. 304 (1994) 249.
[68] X. Su, R.Y. Shen, G.A. Somorjai, Chem. Phys. Lett. 280 (1997) 302.
[69] M.B. Hugenschmidt, A.L. Diaz, C.T. Campbell, J. Phys. Chem. 96 (1992) 5974.
[70] P. Reyes, M. Oportus, G. Pecchi, R. Fréty, B. Moraweck, Catal. Lett. 37 (1996) 193.
[71] J. Barbier, E. Churin, J.M. Parera, J. Riviere, React. Kinet. Catal. Lett. 29 (1985) 323.